Chapter 5

# Cross-Diffusion, Viscous Dissipation and Radiation Effects on an Exponentially Stretching Surface in Porous Media

Ahmed A. Khidir and Precious Sibanda

Additional information is available at the end of the chapter

http://dx.doi.org/10.5772/55320

## 1. Introduction

In the last few decades, fluid flow with heat and mass transfer on a continuously stretching surface has attracted considerable attention because of its many applications in industrial and manufacturing processes. Examples of these applications include the drawing of plastic films, glass-fibre and paper production, hot rolling and continuous casting of metals and spinning of fibers. The kinematics of stretching and the simultaneous heating or cooling during such processes play an important role on the structure and quality of the final product.

Sakiadis [30, 31] was the first to study the boundary layer flow due to a continuous moving solid surface. Subsequently, a huge number of studies dealing with different types of fluids, different forms of stretching velocity and temperature distributions have appeared in the literature. Ali [2] investigated similarity solutions of laminar boundary-layer equations in a quiescent fluid driven by a stretched sheet subject to fluid suction or injection. Elbashbeshy [13] extended this problem to a three dimensional exponentially continuous stretching surface. The problem of an exponentially stretching surface with an exponential temperature distribution has been discussed by Magyari and Keller [19]. The problem of mixed convection from an exponentially stretching surface was studied by Partha et al. [24]. They considered the effect of buoyancy and viscous dissipation in the porous medium. They observed that these had a significant effect on the skin friction and the rate of heat transfer. This problem has been extended by Sajid and Hayat [28] who investigated heat transfer over an exponentially stretching sheet in the presence of heat radiation. The same problem was solved numerically by Bidin and Nazar [6] using the Keller-box method. Flow and heat transfer along an exponentially stretching continuous surface with an exponential temperature distribution and an applied magnetic field has been investigated numerically by

Al-Odat et al. [1] while Khan [17] and Sanjayanand and Khan [29] investigated heat transfer due to an exponentially stretching sheet in a viscous-elastic fluid.

Thermal-diffusion and diffusion-thermo effects in boundary layer flow due to a vertical stretching surface have been studied by, *inter alia*, Dursunkaya and Worek [10] while MHD effects, injection/suction, heat radiation, Soret and Dufour effects on the heat and mass transfer on a continuously stretching permeable surface was investigated by El-Aziz [12]. He showed that the Soret and Dufour numbers have a significant influence on the velocity, temperature and concentration distributions.

Srinivasacharya and RamReddy [33] analyzed the problem of mixed convection in a viscous fluid over an exponentially stretching vertical surface subject to Soret and Dufour effects. Ishak [15] investigated the effect of radiation on magnetohydrodynamic boundary layer flow of a viscous fluid over an exponentially stretching sheet. Pal [9] analyzed the effects of magnetic field, viscous dissipation and internal heat generation/absorption on mixed convection heat transfer in the boundary layers on an exponentially stretching continuous surface with an exponential temperature distribution. Loganathan et al. [18] investigated the effect of a chemical reaction on unsteady free convection flow past a semi-infinite vertical plate with variable viscosity and thermal conductivity. They assumed that the viscosity of the fluid was an exponential function and that the thermal conductivity was a linear function of the temperature. They noted that in the case of variable fluid properties, the results obtained differed significantly from those of constant fluid properties. Javed et al. [16] investigated the non-similar boundary layer flow over an exponentially stretching continuous in rotating flow. They observed a reduction in the boundary layer thickness and an enhanced drag force at the surface with increasing fluid rotation.

The aim of the present study is to investigate the effects of cross-diffusion, chemical reaction, heat radiation and viscous dissipation on an exponentially stretching surface subject to an external magnetic field. The wall temperature, solute concentration and stretching velocity are assumed to be exponentially increasing functions. The successive linearisation method (SLM) which has been used in a limited number of studies (see [3, 5, 20–22, 32]) is used to solve the governing coupled non-linear system of equations. Recent studies such as [4, 22, 23] have suggested that the successive linearisation method is accurate and converges rapidly to the numerical results when compared to other semi-analytical methods such as the Adomian decomposition method, the variational iteration method and the homotopy perturbation method. The SLM method can be used in place of traditional numerical methods such as finite differences, Runge-Kutta shooting methods, finite elements in solving non-linear boundary value problems. We compared the results with the Matlab `bvp4c` numerical routine.

## 2. Governing equations

Consider a quiescent incompressible conducting fluid of constant ambient temperature $T_\infty$ and concentration $C_\infty$ in a porous medium through which an impermeable vertical sheet is stretched with velocity $u_w(x) = u_0 e^{x/\ell}$, temperature distribution $T_w(x) = T_\infty + T_0 e^{2x/\ell}$ and concentration distribution $C_w(x) = C_\infty + C_0 e^{2x/\ell}$ where $C_0$, $T_0$, $u_0$ and $\ell$ are positive constants. The $x$-axis is directed along the continuous stretching surface and the $y$-axis is normal to the surface. A variable magnetic field $B(x)$ is applied in the $y$-direction. In

http://dx.doi.org/10.5772/55320

addition, heat radiation and cross-diffusion effects are considered to be significant. The governing boundary-layer equations subject to the Boussinesq approximations are

$$\frac{\partial u}{\partial x}+\frac{\partial v}{\partial y}=0, \tag{1}$$

$$u\frac{\partial u}{\partial x}+v\frac{\partial u}{\partial y}=\nu\frac{\partial^2 u}{\partial y^2}+g\beta_T(T-T_\infty)+g\beta_C(C-C_\infty)-\left(\frac{\nu}{K}+\frac{\sigma B^2}{\rho}\right)u, \tag{2}$$

$$u\frac{\partial T}{\partial x}+v\frac{\partial T}{\partial y}=\frac{k}{\rho c_p}\frac{\partial^2 T}{\partial y^2}+\frac{\nu}{c_p}\left(\frac{\partial u}{\partial y}\right)^2+\frac{D_m K_T}{c_s c_p}\frac{\partial^2 C}{\partial y^2}-\frac{1}{\rho c_p}\frac{\partial q_r}{\partial y}, \tag{3}$$

$$u\frac{\partial C}{\partial x}+v\frac{\partial C}{\partial y}=D_m\frac{\partial^2 C}{\partial y^2}+\frac{D_m K_T}{T_m}\frac{\partial^2 T}{\partial y^2}-\gamma(C-C_\infty), \tag{4}$$

The boundary conditions are given by

$$\left.\begin{array}{l} u=u_w(x), v=0, T=T_w(x), C=C_w(x) \quad \text{at} \quad y=0, \\ u\to 0, T\to T_\infty, C\to C_\infty \quad \text{as} \quad y\to\infty. \end{array}\right\} \tag{5}$$

where $u$ and $v$ are the velocity components along the $x$ and $y$ axis, respectively, $T$ and $C$ denote the temperature and concentration, respectively, $K$ is the permeability of the porous medium, $\nu$ is the kinematic viscosity, $g$ is the acceleration due to gravity, $\beta_T$ is the coefficient of thermal expansion, $\beta_C$ is the coefficient of concentration expansion, $B$ is the uniform magnetic field, $\rho$ is the liquid density, $\sigma$ is the electrical conductivity, $D_m$ is the mass diffusivity, $c_s$ is the concentration susceptibility, $c_p$ is the specific heat capacity, $T_m$ is the mean fluid temperature, $K_T$ is the thermal diffusion ratio and $\gamma$ is the rate of chemical reaction.

The radiative heat flux term $q_r$ is given by the Rosseland approximation (see Raptis [26] and Sparrow [27]);

$$q_r=-\frac{4\sigma^*}{3k^*}\frac{\partial T^4}{\partial y}, \tag{6}$$

where $\sigma^*$ and $k^*$ are the Stefan-Boltzman constant and the mean absorption coefficient, respectively. We assume that the term $T^4$ may be expanded in a Taylor series about $T_\infty$ and neglecting higher-order terms to get

$$T^4\cong 4T_\infty^3 T-3T_\infty^4, \tag{7}$$

Substituting equations (6) and (7) in equation (3) gives

$$u\frac{\partial T}{\partial x}+v\frac{\partial T}{\partial y}=\left(\frac{k}{\rho c_p}+\frac{16\sigma^* T_\infty^3}{3\rho c_p k^*}\right)\frac{\partial^2 T}{\partial y^2}+\frac{\nu}{c_p}\left(\frac{\partial u}{\partial y}\right)^2+\frac{D_m K_T}{c_s c_p}\frac{\partial^2 C}{\partial y^2}, \tag{8}$$

A similarity solutions may be obtained by assuming that the magnetic field term $B(x)$ has the form

$$B(x) = B_0 e^{x/2\ell} \tag{9}$$

where $B_0$ is the constant magnetic field. The system of partial differential equations (1) - (4) and (8) can be simplified further by introducing the stream function $\psi$ where

$$u = \frac{\partial \psi}{\partial y} \quad \text{and} \quad v = -\frac{\partial \psi}{\partial x}, \tag{10}$$

together with transformations

$$\left.\begin{array}{l} \eta = \dfrac{y}{L}\sqrt{\dfrac{Re}{2}}\, e^{x/2\ell}, \psi = \sqrt{2Re}v\; e^{x/2\ell} f(\eta), \\ T = T_\infty + T_0 e^{2x/\ell}\theta(\eta), C = C_\infty + C_0 e^{2x/\ell}\phi(\eta) \end{array}\right\}. \tag{11}$$

Substituting (11) into the governing partial differential equations gives

$$f''' + ff'' - 2f'^2 - \left(M + \frac{1}{Re_D}\right) f' + 2\frac{Gr_x}{Re^2}\left(\theta + N_1\phi\right) = 0, \tag{12}$$

$$\frac{1}{Pr}\left(1 + \frac{4}{3}R_d\right)\theta'' + f\theta' - 4f'\theta + Gb(f'')^2 + D_f\phi'' = 0, \tag{13}$$

$$\frac{1}{Sc}\phi'' + f\phi' - 4f'\phi + Sr\theta'' - 2R\phi = 0. \tag{14}$$

The corresponding dimensionless boundary conditions take the form

$$\left.\begin{array}{l} f(\eta) = 0,\; f'(\eta) = 1,\; \theta(\eta) = 1,\; \phi(\eta) = 1 \quad \text{at} \quad \eta = 0 \\ f'(\eta) \to 0,\; \theta(\eta) \to 0,\; \phi(\eta) \to 0 \quad \text{as} \quad \eta \to \infty \end{array}\right\} \tag{15}$$

where $M$ is the magnetic parameter, $Gr_x$ is the Grashof number $Re$ is the Reynolds number, $N_1$ is the buoyancy ratio, $Re_D$ is the Darcy-Reynolds number, $Da$ is the Darcy number, $Pr$ is the Prandtl number, $R_d$ is the thermal radiation parameter, $Gb$ is the viscous dissipation parameter or Gebhart number, $D_f$ is the Dufour number, $Sc$ is the Schmidt number, $S_r$ is the Soret number and $R$ is the chemical reaction rate parameter. These parameters are defined as

$$M = \frac{2\sigma B_0^2 \ell}{\rho u_0}, \quad Gr_x = \frac{g\beta_T T_0 \ell^3 e^{2x/\ell}}{\nu^2}, \quad Re = \frac{u_w \ell}{\nu}, \quad N_1 = \frac{\beta_c C_0}{\beta_T T_0}, \tag{16}$$

$$Re_D = \frac{2}{ReDa}, \quad Da = \frac{K}{\ell^2}, \quad Pr = \frac{\nu}{\alpha}, \quad R_d = \frac{4\sigma^* T_\infty^3}{kk^*}, \quad Gb = \frac{u_0^2}{c_p\, T_0}, \tag{17}$$

$$D_f = \frac{D_m K_T C_0}{c_s c_p \nu T_0}, \quad Sc = \frac{\nu}{D_m}, \quad S_r = \frac{D_m K_T T_0}{T_m \nu C_0}, \quad R = \frac{\alpha \ell}{u_0}. \tag{18}$$

http://dx.doi.org/10.5772/55320

The ratio $Gr_x/Re^2$ in equation (12) is the mixed convection parameter which represents aiding buoyancy if $Gr_x/Re^2 > 0$ and opposing buoyancy if $Gr_x/Re^2 < 0$. The skin friction coefficient $C_{fx}$, the Nusselt number $Nu_x$ and the Sherwood $Sh_x$ number are given by

$$C_{fx} = \frac{2\mu}{\rho u_w^2} \left.\frac{\partial u}{\partial y}\right|_{y=0} = \sqrt{\frac{2x}{\ell\, Re_x}}\, f''(0), \tag{19}$$

$$Nu_x = -\frac{x}{T_w - T_\infty} \left.\frac{\partial T}{\partial y}\right|_{y=0} = -\sqrt{\frac{xRe_x}{2\ell}}\, \theta'(0) \tag{20}$$

$$Sh_x = -\frac{x}{C_w - C_\infty} \left.\frac{\partial C}{\partial y}\right|_{y=0} = -\sqrt{\frac{xRe_x}{2\ell}}\, \phi'(0) \tag{21}$$

where $Re_x = xu_w(x)/\nu$ is the local Reynolds number.

## 3. Method of solution

The system of equations (12)-(14) together with the boundary conditions (15) were solved using a successive linearisation method (SLM) (see [22, 32]). The SLM is based on the assumption that the unknown functions $f(\eta)$, $\theta(\eta)$ and $\phi(\eta)$ can be expanded as

$$f(\eta) = f_i(\eta) + \sum_{m=0}^{i-1} F_m(\eta), \theta(\eta) = \theta_i(\eta) + \sum_{m=0}^{i-1} \Theta_m(\eta), \phi(\eta) = \phi_i(\eta) + \sum_{m=0}^{i-1} \Phi_m(\eta), \tag{22}$$

where $f_i$, $\theta_i$ and $\phi_i$ are unknown functions and $F_m$, $\Theta_m$ and $\Phi_m$ $(m \geq 1)$ are successive approximations which are obtained by recursively solving the linear part of the equation system that results from substituting firstly expansions in the governing equations. The initial guesses $F_0(\eta)$, $\Theta_0(\eta)$ and $\Phi_0(\eta)$ are chosen to satisfy the boundary condition

$$\left.\begin{array}{l} F_0(\eta) = 0,\ F_0'(\eta) = 1,\ \Theta_0(\eta) = 1,\ \Phi_0(\eta) = 1 \quad \text{at} \quad \eta = 0 \\ F_0'(\eta) \to 0,\ \Theta_0(\eta) \to 0,\ \Phi_0(\eta) \to 0 \quad \text{as} \quad \eta \to \infty \end{array}\right\}. \tag{23}$$

Suitable choices in this problem are

$$F_0(\eta) = 1 - e^{-\eta},\ \Theta_0(\eta) = e^{-\eta} \quad \text{and} \quad \Phi_0(\eta) = e^{-\eta}. \tag{24}$$

Starting from the initial guesses, the subsequent solutions $F_i$, $\Theta_i$ and $\Phi_i$ $(i \geq 1)$ are obtained by successively solving the linearised form of the equations which are obtained by substituting equation (22) in the governing equations. The linearised equations to be solved are

$$a_{1,i-1}F_i''' + a_{2,i-1}F_i'' + a_{3,i-1}F_i' + a_{4,i-1}F_i + a_{5,i-1}\Theta_i + a_{6,i-1}\Phi_i = r_{1,i-1}, \tag{25}$$

$$b_{1,i-1}\Theta_i'' + b_{2,i-1}\Theta_i' + b_{3,i-1}\Theta_i + b_{4,i-1}F_i'' + b_{5,i-1}F_i' + b_{6,i-1}F_i + b_{7,i-1}\Phi_i = r_{2,i-1}, \tag{26}$$

$$c_{1,i-1}\Phi_i'' + c_{2,i-1}\Phi_i' + c_{3,i-1}\Phi_i + c_{4,i-1}F_i' + c_{5,i-1}F_i + c_{6,i-1}\Theta_i'' = r_{3,i-1}. \tag{27}$$

subject to the boundary conditions

$$F_i(0) = F_i'(0) = F_i'(\infty) = \Theta_i(0) = \Theta_i(\infty) = \Phi_i(0) = \Phi_i(\infty) = 0, \tag{28}$$

where the coefficient parameters are

$$a_{1,i-1} = -1, \quad a_{2,i-1} = \sum_{m=0}^{i-1} f_m', \quad a_{3,i-1} = -4\sum_{m=0}^{i-1} f_m' - M - \frac{1}{Re_D}, a_{4,i-1} = \sum_{m=0}^{i-1} f_m''$$

$$a_{5,i-1} = 2\frac{Gr_x}{Re^2},\ a_{6,i-1} = 2N_1\frac{Gr_x}{Re^2},\ b_{1,i-1} = \sum_{m=0}^{i-1} f_m,\ b_{2,i-1} = -4\sum_{m=0}^{i-1} \theta_m, b_{3,i-1} = \sum_{m=0}^{i-1} \theta_m',$$

$$b_{4,i-1} = \frac{3+4R_d}{3Pr},\ b_{5,i-1} = \sum_{m=0}^{i-1} f_m,\ b_{6,i-1} = -4\sum_{m=0}^{i-1} f_m',\ b_{7,i-1} = D_f,\ c_{1,i-1} = -4\sum_{m=0}^{i-1} \phi_m$$

$$c_{2,i-1} = \sum_{m=0}^{i-1} \phi_m',\ c_{3,i-1} = Sr,\ c_{4,i-1} = \frac{1}{Sc},\ c_{5,i-1} = \sum_{m=0}^{i-1} f_m,\ c_{6,i-1} = -2R - 4\sum_{m=0}^{i-1} f_m',$$

$$r_{1,i-1} = -\sum_{m=0}^{i-1} f_m''' - \sum_{m=0}^{i-1} f_m \sum_{m=0}^{i-1} f_m'' + 2\sum_{m=0}^{i-1} f_m'^2 + \left(M + \frac{1}{Re_D}\right)\sum_{m=0}^{i-1} f_m'$$
$$-\frac{2Gr_x}{Re^2}\sum_{m=0}^{i-1}(\theta_m + N_1\phi_m)$$

$$r_{2,i-1} = -\sum_{m=0}^{i-1}\frac{1}{Pr}(\phi_m'' + \frac{4R_d}{3Pr}\theta_m'') - \sum_{m=0}^{i-1} f_m \sum_{m=0}^{i-1}\theta_m' + 4\sum_{m=0}^{i-1} f_m' \sum_{m=0}^{i-1}\theta_m - Gb\sum_{m=0}^{i-1} f_m''^2 -$$
$$D_f\sum_{m=0}^{i-1}\phi_m''$$

$$r_{3,i-1} = -\frac{1}{Sc}\sum_{m=0}^{i-1}\phi_m'' \sum_{m=0}^{i-1} f_m \sum_{m=0}^{i-1}\phi_m' + 4\sum_{m=0}^{i-1} f_m \sum_{m=0}^{i-1}\theta_m - Sr\sum_{m=0}^{i-1}\phi_m'' + 2R\sum_{m=0}^{i-1}\phi_m$$

The solutions $F_i$, $\Theta_i$ and $\Phi_i$ for $i \geq 1$ are found by iteratively solving equations (25)-(27). Finally, after $M$ iterations, the solutions $f(\eta)$, $\theta(\eta)$ and $\phi(\eta)$ may be written as

$$f(\eta) \approx \sum_{m=0}^{M} F_m(\eta), \theta(\eta) \approx \sum_{m=0}^{M} \Theta_m(\eta), \Phi(\eta) \approx \sum_{m=0}^{M} \Phi_m(\eta). \tag{29}$$

where $M$ is termed the order of SLM approximation. Equations (25)-(27) are solved using the Chebyshev spectral collocation method. We first transform the domain of solution $[0, \infty)$ into the domain $[-1, 1]$ using the domain truncation technique where the problem is solved

http://dx.doi.org/10.5772/55320

in the interval $[0, L]$ where $L$ is a scaling parameter used to invoke the boundary condition at infinity. This is achieved by using the mapping

$$\frac{\eta}{L} = \frac{\xi + 1}{2}, -1 \leq \xi \leq 1, \tag{30}$$

We discretize the domain $[-1, 1]$ using the Gauss-Lobatto collocation points given by

$$\xi = \cos\frac{\pi j}{N}, j = 0, 1, 2, \ldots, N, \tag{31}$$

where $N$ is the number of collocation points used. The functions $F_i$, $\Theta_i$ and $\Phi_i$ for $i \geq 1$ are approximated at the collocation points as follows

$$F_i(\xi) \approx \sum_{k=0}^{N} F_i(\xi_k)T_k(\xi_j), \Theta_i(\xi) \approx \sum_{k=0}^{N} \Theta_i(\xi_k)T_k(\xi_j), \Phi_i(\xi) \approx \sum_{k=0}^{N} \Phi_i(\xi_k)T_k(\xi_j) j = 0, 1, \ldots, N, \tag{32}$$

where $T_k$ is the $k^{\text{th}}$ Chebyshev polynomial given by

$$T_k(\xi) = \cos\left[k\cos^{-1}(\xi)\right]. \tag{33}$$

The derivatives of the variables at the collocation points are represented as

$$\frac{d^r F_i}{d\eta^r} = \sum_{k=0}^{N} \mathbf{D}_{kj}^r F_i(\xi_k), \frac{d^r \Theta_i}{d\eta^r} = \sum_{k=0}^{N} \mathbf{D}_{kj}^r \Theta_i(\xi_k), \frac{d^r \Phi_i}{d\eta^r} = \sum_{k=0}^{N} \mathbf{D}_{kj}^r \Phi_i(\xi_k) j = 0, 1, \ldots, N, \tag{34}$$

where $r$ is the order of differentiation and $\mathbf{D} = \frac{2}{L}\mathcal{D}$ with $\mathcal{D}$ being the Chebyshev spectral differentiation matrix (see, for example [7, 8]), whose entries are defined as

$$\left.\begin{aligned} \mathcal{D}_{00} &= \frac{2N^2+1}{6}, \\ \mathcal{D}_{jk} &= \frac{c_j}{c_k}\frac{(-1)^{j+k}}{\xi_j - \xi_k}, j \neq k; j, k = 0, 1, \ldots, N, \\ \mathcal{D}_{kk} &= -\frac{\xi_k}{2(1-\xi_k^2)}, k = 1, 2, \ldots, N-1, \\ \mathcal{D}_{NN} &= -\frac{2N^2+1}{6}. \end{aligned}\right\} \tag{35}$$

Substituting equations (30)-(34) into equations (25)-(27) leads to the matrix equation

$$\mathbf{A}_{i-1}\mathbf{X}_i = \mathbf{R}_{i-1}, \tag{36}$$

In equation (36), $\mathbf{A}_{i-1}$ is a $(3N+3)\times(3N+3)$ square matrix and $\mathbf{X}_i$ and $\mathbf{R}_{i-1}$ are $(3N+3)\times 1$ column vectors defined by

$$\mathbf{A}_{i-1}=\begin{bmatrix} A_{11} & A_{12} & A_{13}\\ A_{21} & A_{22} & A_{23}\\ A_{31} & A_{32} & A_{33}\end{bmatrix}, \mathbf{X}_i=\begin{bmatrix} F_i\\ \Theta_i\\ \Phi_i\end{bmatrix}, \mathbf{R}_{i-1}=\begin{bmatrix} \mathbf{r}_{1,i-1}\\ \mathbf{r}_{2,i-1}\\ \mathbf{r}_{3,i-1}\end{bmatrix}, \tag{37}$$

where

$$\begin{aligned}
&F_i=[f_i(\xi_0),f_i(\xi_1),...,f_i(\xi_{N-1}),f_i(\xi_N)]^T,\\
&\Theta_i=[\theta_i(\xi_0),\theta_i(\xi_1),...,\theta_i(\xi_{N-1}),\theta_i(\xi_N)]^T,\\
&\Phi_i=[\phi_i(\xi_0),\phi_i(\xi_1),...,\phi_i(\xi_{N-1}),\phi_i(\xi_N)]^T,\\
&\mathbf{r}_{1,i-1}=\left[r_{1,i-1}(\xi_0),r_{1,i-1}(\xi_1),...,r_{1,i-1}(\xi_{N-1}),r_{1,i-1}(\xi_N)\right]^T,\\
&\mathbf{r}_{2,i-1}=\left[r_{2,i-1}(\xi_0),r_{2,i-1}(\xi_1),...,r_{2,i-1}(\xi_{N-1}),r_{2,i-1}(\xi_N)\right]^T,\\
&\mathbf{r}_{3,i-1}=\left[r_{3,i-1}(\xi_0),r_{3,i-1}(\xi_1),...,r_{3,i-1}(\xi_{N-1}),r_{3,i-1}(\xi_N)\right]^T,\\
&A_{11}=\mathbf{a}_{1,i-1}\mathbf{D}^3+\mathbf{a}_{2,i-1}\mathbf{D}^2+\mathbf{a}_{3,i-1}\mathbf{D}+\mathbf{a}_{4,i-1}\mathbf{I}, A_{12}=\mathbf{a}_{5,i-1}\mathbf{I}+\mathbf{a}_{6,i-1}\mathbf{I}, A_{13}=\mathbf{I},\\
&A_{21}=\mathbf{b}_{1,i-1}\mathbf{D}^2+\mathbf{b}_{2,i-1}\mathbf{D}+\mathbf{b}_{3,i-1}\mathbf{I}, A_{22}=\mathbf{b}_{4,i-1}\mathbf{D}^2+\mathbf{b}_{5,i-1}\mathbf{D}+\mathbf{b}_{6,i-1}\mathbf{I}, A_{23}=\mathbf{b}_{7,i-1}\mathbf{D}^2,\\
&A_{31}=\mathbf{c}_{1,i-1}\mathbf{D}^2+\mathbf{c}_{2,i-1}\mathbf{D}+\mathbf{c}_{3,i-1}\mathbf{I}, A_{32}=\mathbf{c}_{4,i-1}\mathbf{D}+\mathbf{c}_{5,i-1}\mathbf{I}, A_{33}=\mathbf{c}_{6,i-1}\mathbf{D}^2.
\end{aligned}$$

In the above definitions $T$ stands for transpose, $\mathbf{a}_{k,i-1}$ $(k=1,\ldots,6)$, $\mathbf{b}_{k,i-1}$ $(k=1,\ldots,7)$, $\mathbf{c}_{k,i-1}$ $(k=1,\ldots,6)$, and $\mathbf{r}_{k,i-1}$ $(k=1,2,3)$ are diagonal matrices of order $(N+1)\times(N+1)$, $\mathbf{I}$ is an identity matrix of order $(N+1)\times(N+1)$. Finally the solution is obtained as

$$\mathbf{X}_i=\mathbf{A}_{i-1}^{-1}\mathbf{R}_{i-1}. \tag{38}$$

## 4. Results and discussion

In generating the results presented here it was determined through numerical experimentation that $L=15$ and $N=60$ gave sufficient accuracy for the linearisation method. In addition, the results in this work were obtained for $Pr=0.71$ which physically corresponds to air and the Schmidt number $Sc=0.22$ for hydrogen at approximately 25° and one atmospheric pressure. The Darcy-Reynolds number was fixed at $Re_D=100$.

Tables 1 - 7 show, firstly the effects of various parameters on the skin-friction, the local heat and the mass transfer coefficients for different physical parameters values. Secondly, to confirm the accuracy of the linearisation method, these results are compared to those obtained using the Matlab `bvp4c` solver. The results from the two methods are in excellent agreement with the linearisation method converging at the four order with accuracy of up to six decimal places.

The effect of increasing the magnetic filed parameter $M$ on the skin-friction coefficient $f''(0)$, the Nusselt number $-\theta'(0)$ and the Sherwood number $-\phi'(0)$ are given in Table 1. Here

http://dx.doi.org/10.5772/55320

we find that increasing the magnetic filed parameter leads to reduces Nusselt number and Sherwood number as well as skin friction coefficient in case of aiding buoyancy. These results are to be expected, and are, in fact, similar to those obtained previously by, among others (Ishak [15] and Ibrahim and Makinde [14]).

| | | **SLM results** | | | | |
|---|---|---|---|---|---|---|
| | $M$ | 1st order | 2nd order | 3rd order | 4th order | **bvp4c** |
| $f''(0)$ | 0.0 | -0.130330 | -0.137803 | -0.138236 | -0.138242 | -0.138242 |
| | 0.1 | -0.172947 | -0.179731 | -0.179950 | -0.179952 | -0.179952 |
| | 0.5 | -0.334846 | -0.339272 | -0.339242 | -0.339242 | -0.339242 |
| | 1.0 | -0.521003 | -0.523599 | -0.523568 | -0.523568 | -0.523568 |
| $-\theta'(0)$ | 0.0 | 1.422819 | 1.354658 | 1.354263 | 1.354252 | 1.354252 |
| | 0.1 | 1.407222 | 1.345231 | 1.345006 | 1.345004 | 1.345003 |
| | 0.5 | 1.349392 | 1.308530 | 1.308480 | 1.308480 | 1.308480 |
| | 1.0 | 1.286198 | 1.264064 | 1.264037 | 1.264037 | 1.264037 |
| $-\phi'(0)$ | 0.0 | 1.297706 | 1.288178 | 1.288065 | 1.288063 | 1.288063 |
| | 0.1 | 1.294285 | 1.285273 | 1.285212 | 1.285212 | 1.285212 |
| | 0.5 | 1.281653 | 1.274574 | 1.274572 | 1.274572 | 1.274572 |
| | 1.0 | 1.267871 | 1.262761 | 1.262760 | 1.262760 | 1.262760 |

**Table 1.** The effect of various values of $M$ on skin-friction, heat and mass transfer coefficients when $Gr_x/Re^2 = 1.5$, $Gb = 0.5$, $R_d = 0.2$, $D_f = 0.3$, $Sr = 0.2$, $R = 2$ and $N_1 = 0.1$

In Table 2 an increase in the mixed convection parameter $Gr_x/Re^2$ (that is, aiding buoyancy) enhances the skin friction coefficient. This is explained by the fact that an increase in the fluid buoyancy leads to an acceleration of the fluid flow, thus increasing the skin friction coefficient. Similar results were obtained in the past by Srinivasacharya and RamReddy [33] and Partha et al. [24]. Also, the non-dimensional heat and mass transfer coefficients increase when $Gr_x/Re^2$ increases. This is because an increasing in mixed convection parameter, increases the momentum transport in the boundary layer this is leads to carried out more heat and mass species out of the surface, then reducing the thermal and concentration boundary layers thickness and hence increasing the heat and mass transfer rates.

Tables 3 and 4 show the effects of increasing the radiation parameter $R_d$ and the chemical reaction parameter $R$ on the skin-friction, and the heat and mass transfer rates respectively. The skin-friction coefficient is enhanced by the radiation parameter. It is however reduced by the chemical reaction parameter (Loganathan et. al[18]). Increasing the radiation parameter $R_d$ and chemical reaction parameter $R$ have the same effect on heat and mass transfer rates, that is, $-\theta'(0)$ decreases while $-\phi'(0)$ is increases. Large values of $R_d$ and $R$ lead to a decrease in the buoyancy force and, consequently, a decrease in the thicknesses of both the thermal and the momentum boundary layers (see Sajid [28]).

| | | SLM results | | | | |
|---|---|---|---|---|---|---|
| | $Gr_x/Re^2$ | 1st order | 2nd order | 3rd order | 4th order | **bvp4c** |
| $f''(0)$ | 0.0 | -1.459148 | -1.469821 | -1.469885 | -1.469885 | -1.469885 |
| | 0.5 | -1.042194 | -1.044162 | -1.044208 | -1.044208 | -1.044208 |
| | 1.0 | -0.674522 | -0.678490 | -0.678447 | -0.678447 | -0.678447 |
| | 1.5 | -0.334846 | -0.339272 | -0.339242 | -0.339242 | -0.339242 |
| $-\theta'(0)$ | 0.0 | 0.973213 | 0.934517 | 0.933372 | 0.933372 | 0.933372 |
| | 0.5 | 1.135051 | 1.134112 | 1.134083 | 1.134083 | 1.134083 |
| | 1.0 | 1.253215 | 1.236804 | 1.236738 | 1.236738 | 1.236738 |
| | 1.5 | 1.349392 | 1.308530 | 1.308480 | 1.308480 | 1.308480 |
| $-\phi'(0)$ | 0.0 | 1.200469 | 1.201715 | 1.201709 | 1.201709 | 1.201709 |
| | 0.5 | 1.234639 | 1.233314 | 1.233299 | 1.233299 | 1.233299 |
| | 1.0 | 1.260335 | 1.255659 | 1.255655 | 1.255655 | 1.255655 |
| | 1.5 | 1.281653 | 1.274574 | 1.274572 | 1.274572 | 1.274572 |

**Table 2.** The effect of various values of $Gr_x/Re^2$ on skin-friction, heat and mass transfer coefficients when $M = 0.5,\ Gb = 0.5,\ R_d = 0.2,\ D_f = 0.3,\ Sr = 0.2,\ R = 2$ and $N_1 = 0.1$

| | | SLM results | | | | |
|---|---|---|---|---|---|---|
| | $R_d$ | 1st order | 2nd order | 3rd order | 4th order | **bvp4c** |
| $f''(0)$ | 0.0 | -0.390151 | -0.384799 | -0.385087 | -0.385088 | -0.385088 |
| | 0.2 | -0.334846 | -0.339272 | -0.339242 | -0.339242 | -0.339242 |
| | 0.5 | -0.267055 | -0.286928 | -0.286715 | -0.286715 | -0.286715 |
| | 1.0 | -0.178534 | -0.223773 | -0.224247 | -0.224239 | -0.224239 |
| $-\theta'(0)$ | 0.0 | 1.508929 | 1.466549 | 1.466541 | 1.466540 | 1.466540 |
| | 0.2 | 1.349392 | 1.308530 | 1.308480 | 1.308480 | 1.308480 |
| | 0.5 | 1.184709 | 1.146728 | 1.146321 | 1.146321 | 1.146321 |
| | 1.0 | 1.008715 | 0.976294 | 0.974693 | 0.974674 | 0.974674 |
| $-\phi'(0)$ | 0.0 | 1.267312 | 1.263619 | 1.263567 | 1.263567 | 1.263567 |
| | 0.2 | 1.281653 | 1.274574 | 1.274572 | 1.274572 | 1.274572 |
| | 0.5 | 1.298805 | 1.286546 | 1.286483 | 1.286483 | 1.286483 |
| | 1.0 | 1.320928 | 1.300398 | 1.299833 | 1.299832 | 1.299832 |

**Table 3.** The effect of $R_d$ on skin-friction, heat and mass transfer coefficients when $M = 0.5,\ Gr_x/Re^2 = 1.5,\ Gb = 0.5,\ D_f = 0.3,\ Sr = 0.2,\ R = 2$ and $N_1 = 0.1$

http://dx.doi.org/10.5772/55320

| | | SLM results | | | | |
|---|---|---|---|---|---|---|
| | $R$ | 1st order | 2nd order | 3rd order | 4th order | **bvp4c** |
| $f''(0)$ | 0.0 | -0.332793 | -0.334754 | -0.334629 | -0.334629 | -0.334629 |
| | 0.5 | -0.333949 | -0.336858 | -0.336797 | -0.336797 | -0.336797 |
| | 1.0 | -0.334431 | -0.337995 | -0.337952 | -0.337952 | -0.337952 |
| | 3.0 | -0.334965 | -0.339959 | -0.339936 | -0.339936 | -0.339936 |
| $-\theta'(0)$ | 0.0 | 1.413844 | 1.364409 | 1.364235 | 1.364232 | 1.364232 |
| | 0.5 | 1.392460 | 1.347513 | 1.347472 | 1.347472 | 1.347472 |
| | 1.0 | 1.376336 | 1.333290 | 1.333247 | 1.333247 | 1.333247 |
| | 3.0 | 1.326247 | 1.286737 | 1.286682 | 1.286682 | 1.286682 |
| $-\phi'(0)$ | 0.0 | 0.773109 | 0.807913 | 0.809416 | 0.809448 | 0.809448 |
| | 0.5 | 0.950211 | 0.956980 | 0.957025 | 0.957025 | 0.957025 |
| | 1.0 | 1.076976 | 1.076044 | 1.076055 | 1.076055 | 1.076055 |
| | 3.0 | 1.452263 | 1.442740 | 1.442734 | 1.442734 | 1.442734 |

**Table 4.** The effect of $R$ on skin-friction, heat and mass transfer coefficients when $M = 0.5$, $Gr_x/Re^2 = 1.5$, $Gb = 0.5$, $R_d = 0.2$, $D_f = 0.3$, $Sr = 0.2$ and $N_1 = 0.1$

Table 5 shows the influence of the viscous dissipation parameter $Gb$. The skin-friction coefficient and the Sherwood number increase as $Gb$ increases. However, the heat transfer rate is reduced when $Gb$ is increased.

The effect of the Soret parameter on the skin-friction, the heat and the mass transfer coefficients is presented in Table 6. Clearly, increasing this parameter leads to increase in the heat transfer rate and a decrease in both the skin friction coefficient and the mass transfer rate. Similar findings were reported by Partha et al. [25].

Table 7 shows the effect of the Dufour number on the skin-friction, the heat and the mass transfer coefficients. It seen that as the Dufour parameter increases, the skin-friction coefficient and mass transfer rate are enhanced while the mass transfer rate is reduced. The Soret and Dufour numbers have opposite effects on Nusselt and Sherwood numbers.

| | | SLM results | | | | |
|---|---|---|---|---|---|---|
| | $Gb$ | 1st order | 2nd order | 3rd order | 4th order | **bvp4c** |
| $f''(0)$ | 0.0 | -0.351301 | -0.354490 | -0.354558 | -0.354558 | -0.354558 |
| | 0.5 | -0.334846 | -0.339272 | -0.339242 | -0.339242 | -0.339242 |
| | 1.0 | -0.320079 | -0.325029 | -0.324930 | -0.324930 | -0.324930 |
| | 2.0 | -0.295309 | -0.299203 | -0.298988 | -0.298988 | -0.298988 |
| $-\theta'(0)$ | 0.0 | 1.364554 | 1.341183 | 1.341179 | 1.341179 | 1.341179 |
| | 0.5 | 1.349392 | 1.308530 | 1.308480 | 1.308480 | 1.308480 |
| | 1.0 | 1.340317 | 1.278965 | 1.278884 | 1.278884 | 1.278883 |
| | 2.0 | 1.337606 | 1.227792 | 1.227640 | 1.227640 | 1.227640 |
| $-\phi'(0)$ | 0.0 | 1.278392 | 1.271621 | 1.271607 | 1.271607 | 1.271607 |
| | 0.5 | 1.281653 | 1.274574 | 1.274572 | 1.274572 | 1.274572 |
| | 1.0 | 1.284491 | 1.277309 | 1.277310 | 1.277310 | 1.277310 |
| | 2.0 | 1.289013 | 1.282196 | 1.282194 | 1.282194 | 1.282194 |

**Table 5.** The effect of $Gb$ on skin-friction, heat and mass transfer coefficients when $M = 0.5,\ Gr_x/Re^2 = 1.5,\ R_d = 0.2,\ D_f = 0.3,\ Sr = 0.2,\ R = 2$ and $N_1 = 0.1$

| | | SLM results | | | | |
|---|---|---|---|---|---|---|
| | $Sr$ | 1st order | 2nd order | 3rd order | 4th order | **bvp4c** |
| $f''(0)$ | 0.1 | -0.271640 | -0.289773 | -0.289559 | -0.289559 | -0.289559 |
| | 0.5 | -0.332574 | -0.337635 | -0.337603 | -0.337603 | -0.337603 |
| | 1.0 | -0.338023 | -0.341848 | -0.341863 | -0.341863 | -0.341863 |
| | 1.5 | -0.338296 | -0.341846 | -0.341878 | -0.341878 | -0.341878 |
| $-\theta'(0)$ | 0.1 | 1.192649 | 1.151536 | 1.151190 | 1.151190 | 1.151190 |
| | 0.5 | 1.343705 | 1.304565 | 1.304512 | 1.304512 | 1.304512 |
| | 1.0 | 1.363632 | 1.324409 | 1.324369 | 1.324369 | 1.324369 |
| | 1.5 | 1.371163 | 1.331565 | 1.331527 | 1.331527 | 1.331527 |
| $-\phi'(0)$ | 0.1 | 1.311432 | 1.298783 | 1.298733 | 1.298733 | 1.298733 |
| | 0.5 | 1.233004 | 1.228589 | 1.228590 | 1.228590 | 1.228590 |
| | 1.0 | 1.146766 | 1.147516 | 1.147516 | 1.147516 | 1.147516 |
| | 1.5 | 1.061229 | 1.066875 | 1.066878 | 1.066878 | 1.066878 |

**Table 6.** The effect of $Sr$ on skin-friction, heat and mass transfer coefficients when $M = 0.5,\ Gr_x/Re^2 = 1.5,\ Gb = 0.5,\ R_d = 0.3,\ R = 2$ and $N_1 = 0.1$

http://dx.doi.org/10.5772/55320

| | | SLM results | | | | |
|---|---|---|---|---|---|---|
| | $D_f$ | 1st order | 2nd order | 3rd order | 4th order | **bvp4c** |
| $f''(0)$ | 0.1 | -0.2897226 | -0.3041903 | -0.3039915 | -0.3039916 | -0.3039916 |
| | 0.3 | -0.2670553 | -0.2869281 | -0.2867154 | -0.2867154 | -0.2867154 |
| | 0.7 | -0.2181199 | -0.2504226 | -0.2503761 | -0.2503747 | -0.2503747 |
| | 1.5 | -0.1168316 | -0.1785689 | -0.1797718 | -0.1797642 | -0.1797642 |
| $-\theta'(0)$ | 0.1 | 1.2407545 | 1.2030266 | 1.2027860 | 1.2027860 | 1.2027860 |
| | 0.3 | 1.1847094 | 1.1467282 | 1.1463211 | 1.1463211 | 1.1463211 |
| | 0.7 | 1.0731585 | 1.0350043 | 1.0341356 | 1.0341344 | 1.0341344 |
| | 1.5 | 0.8462011 | 0.8114925 | 0.8093554 | 0.8093376 | 0.8093375 |
| $-\phi'(0)$ | 0.1 | 1.2343382 | 1.2276842 | 1.2276800 | 1.2276800 | 1.2276800 |
| | 0.3 | 1.2988048 | 1.2865458 | 1.2864829 | 1.2864829 | 1.2864829 |
| | 0.7 | 1.3245499 | 1.3072132 | 1.3069707 | 1.3069708 | 1.3069708 |
| | 1.5 | 1.3489087 | 1.3224155 | 1.3214809 | 1.3214790 | 1.3214790 |

**Table 7.** The effect of $D_f$ on skin-friction, heat and mass transfer coefficients when $M = 0.5$, $Gr_x/Re^2 = 1.5$, $Gb = 0.5$, $R_d = 0.5$, $R = 2$ and $N_1 = 0.1$

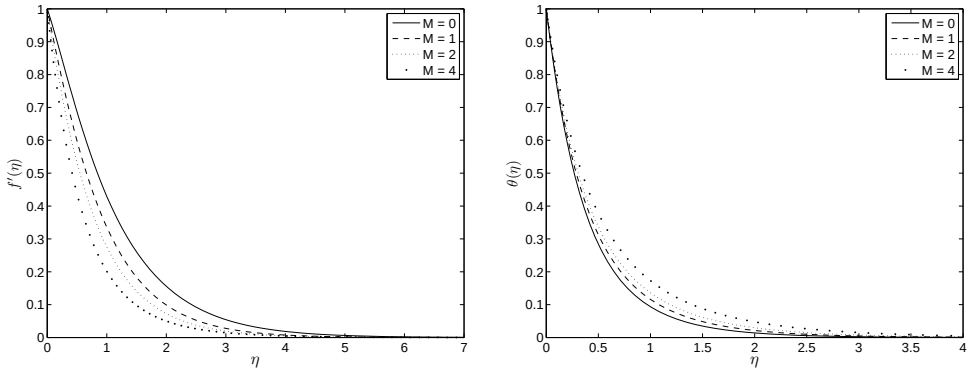


**Figure 1.** Effect of magnetic parameter $M$ on the (a) velocity and, (b) temperature when $Gr_x/Re^2 = 1.5$, $Gb = 0.5$, $R_d = 1$, $D_f = 0.3$, $Sr = 0.2$, $R = 0.1$ and $N_1 = 0.1$

The effects of the various fluid and physical parameters on the fluid properties are displayed qualitatively in Figures 1 - 7. Figure 1 illustrates the effect of the magnetic parameter $M$ on the boundary layer velocity and the temperature within the thermal boundary layer. As expected, we observe that increasing the magnetic filed parameter reduces the velocity due to an increase in the Lorentz force which acts against the flow if the magnetic field is applied in the normal direction. This naturally leads to an increase in the temperature (and concentration) within the boundary layer as less heat is conducted away.

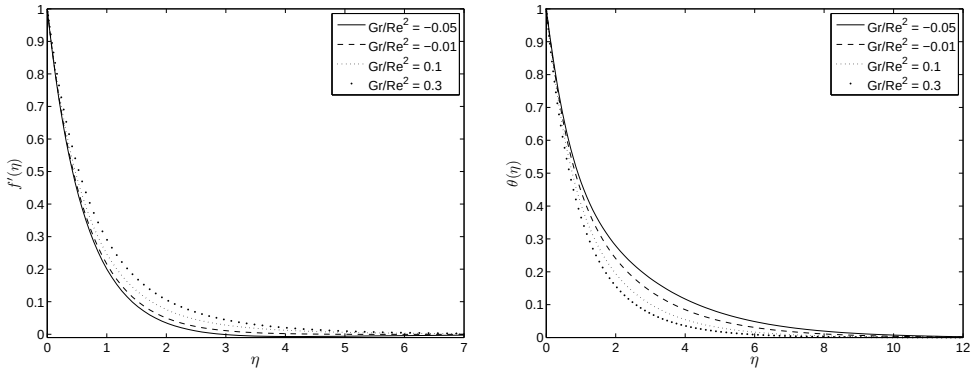


**Figure 2.** Effect of the mixed convection parameter $Gr_x/Re^2$ on the (a) velocity and (b) temperature when $M = 0.1$, $Gb = 0.1$, $R_d = 0.01$, $D_f = 0.3$, $Sr = 0.2$, $R = 0.2$ and $N_1 = 0.1$

Figure 2 shows the dimensionless velocity and temperature for various values of the mixed convection parameter $Gr_x/Re^2$ in the case of both aiding and opposing flow. We note that when the convection parameter increases, the velocity increases (the velocity is higher for aiding flow and less for opposing flow). The temperature (and solute concentration although not shown here) reduces as the convection parameter increases. Similar results were reported by Srinivasacharya and RamReddy [33].

Figure 3 shows the influence of the thermal radiation parameter $R_d$ and the viscous dissipation $Gb$ on the fluid velocity. The velocity increase with increasing thermal radiation parameter

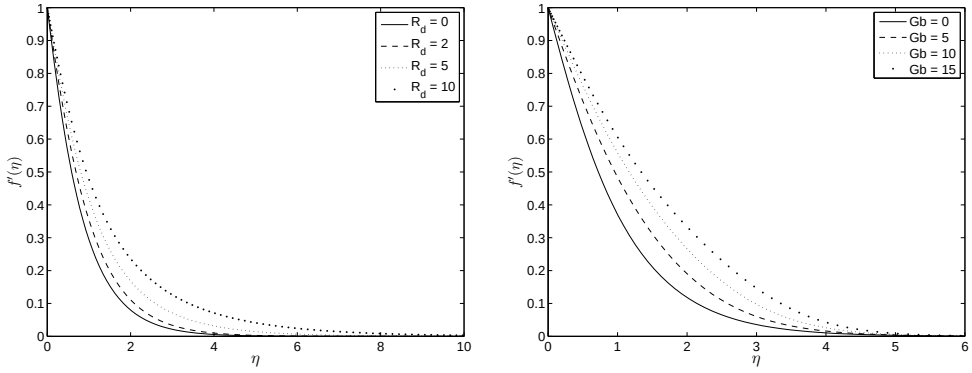


**Figure 3.** Effect of (a) the thermal radiation parameter $R_d$, and (b) viscous dissipation parameter $Gb$ on the fluid velocity when $M = 0.5$, $Gr_x/Re^2 = 1.5$, $Gb = 0.5$, $D_f = 0.3$, $Sr = 0.2$, $R = 0.1$ and $N_1 = 0.1$

Figure 4 shows the influence of the thermal radiation parameter $R_d$ and the viscous dissipation $Gb$ on the temperature within the thermal boundary layer. Naturally, the temperature increases with an increase in the thermal radiation and viscous dissipation parameters.

http://dx.doi.org/10.5772/55320

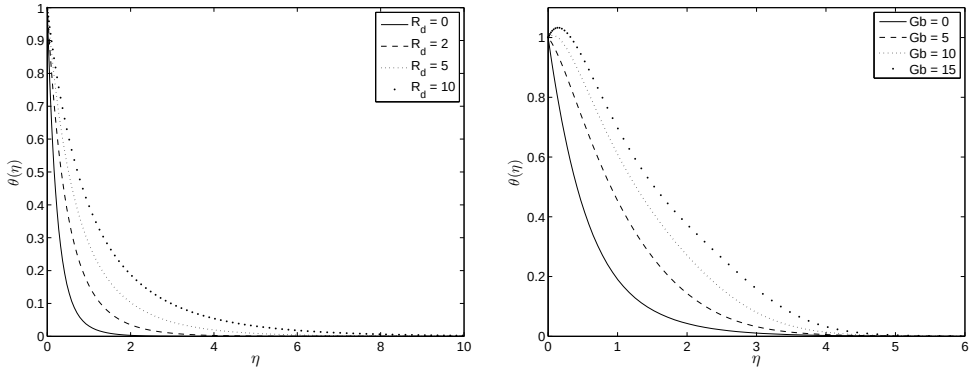


**Figure 4.** Effect of (a) the thermal radiation parameter $R_d$, and (b) viscous dissipation parameter $Gb$ on the temperature within the thermal boundary layer when $M = 0.5,\ Gr_x/Re^2 = 1.5,\ Gb = 0.5,\ D_f = 0.3,\ Sr = 0.2,\ R = 0.1$ and $N_1 = 0.1$

The effect of the viscous dissipation parameter $Gb$ on the solute concentration is shown in Figure 5. The solute concentration decreases with increasing viscous dissipation.

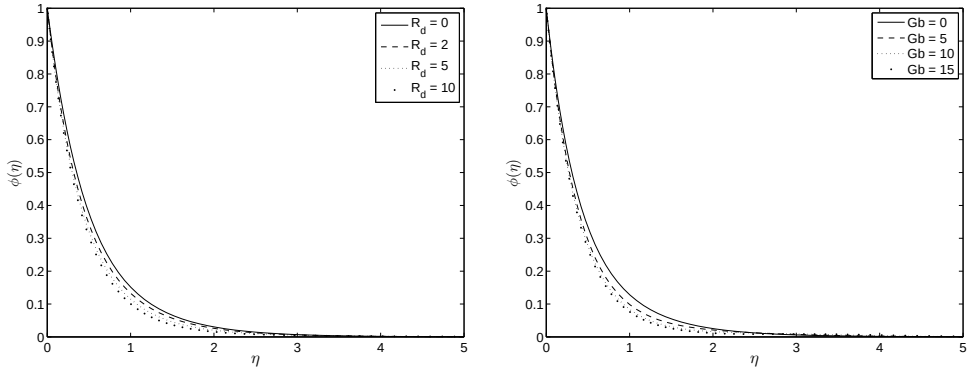


**Figure 5.** Effect of (a) the thermal radiation parameter $R_d$, and (b) the viscous dissipation parameter $Gb$ on the solute concentration when $M = 0.5,\ Gr_x/Re^2 = 1.5,\ R_d = 1,\ D_f = 0.3,\ Sr = 0.2,\ R = 0.1$ and $N_1 = 0.1$

In Figure 6 we show the effect of increasing the Dufour $D_f$ (that is, reducing the Soret $Sr$) parameter on the fluid velocity, temperature and solute concentration, respectively. The fluid velocity is found to increase with both parameters. An increase in $D_f$ enhances the temperature within the thermal boundary layer.

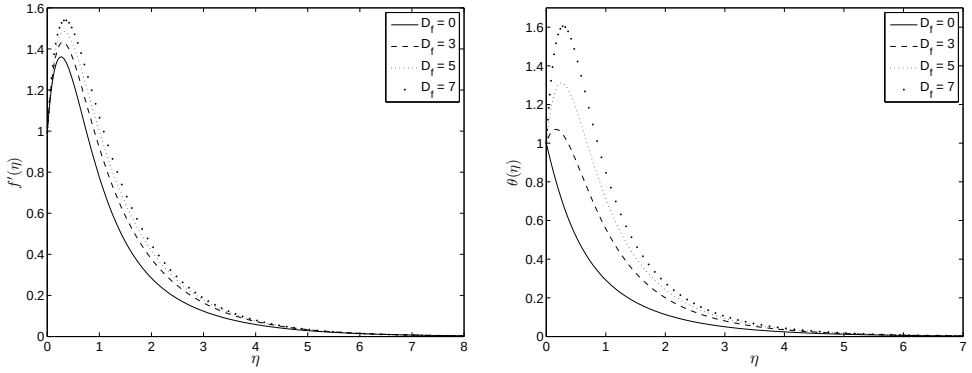


**Figure 6.** Effect of the Dufour number $D_f$ on the (a) velocity, and (b) temperature when $M = 0.5$, $Gr_x/Re^2 = 1.5$, $Gb = 0.5$, $R_d = 0.2$, $R = 0.1$ and $N_1 = 2$

The effect of the chemical reaction parameter $R$ on the fluid properties is shown in Figure 7. We note that the velocity reduces as the chemical reaction parameter $R$ increases. However, the solute concentration within boundary layer naturally decreases with an increase in the chemical reaction.

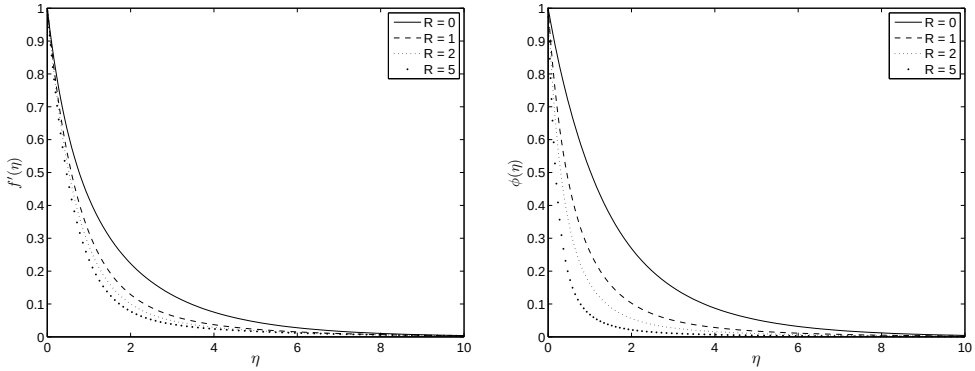


**Figure 7.** Effect of the chemical reaction parameter $R$ on the (a) velocity, and (b) concentration distributions when $M = 2$, $Gr_x/Re^2 = 1.5$, $Gb = 0.5$, $R_d = 1$, $R = 0.1$, $D_f = 0.3$, $Sr = 0.2$ and $N_1 = 5$

## 5. Conclusion

In this chapter we have studied the effects of cross-diffusion and viscous dissipation on heat and mass transfer from an exponentially stretching surface in porous media. We further considered the effects of thermal radiation and a chemical reaction. The governing equations were solved using the successive linearisation method. This has been shown to give accurate results. The effects of various physical parameters on the fluid properties, the skin-friction coefficient and the heat and the mass transfer rates have been determined. It was found, inter alia, that the velocity increase with the mixed convection parameter while the temperature and concentration profiles decrease. An increase in both viscous dissipation and radiation

http://dx.doi.org/10.5772/55320

parameters reduced the concentration distribution while the temperature was enhanced by viscous dissipation and radiation parameters. The skin-friction, heat and mass transfer coefficients decreased with an increase in the magnetic field strength. The skin-friction and mass transfer coefficients decreased whereas the heat transfer coefficient increased with increasing Soret numbers.

## Author details

Ahmed A. Khidir and Precious Sibanda

School of Mathematics, Statistics and Computer Science, University of KwaZulu-Natal, South Africa

## References

[1] Al-Odat, M.Q.; Damseh, R.A. & Al-Azab, T.A. (2006). Thermal boundary layer on an exponentially stretching continuous surface in the presence of magnetic field effect. *Int. J. Appl. Mech. Eng.* 11, pp. 289-299.

[2] Ali, M. E. (1995). On thermal boundary layer on a power law stretched surface with suction or injection. *International Journal of Heat and Fluid Flow*, 16, pp. 280-290.

[3] Awad, F. G.; Sibanda, P.; Motsa, S. S. & Makinde, O. D. (2011). Convection from an inverted cone in a porous medium with cross-diffusion effects. *Computers & Mathematics with Applications*, 61, pp. 1431-1441.

[4] Awad, F. G.; Sibanda, P.; Narayana, M. & Motsa, S. S. (2011). Convection from a semi-finite plate in a fluid saturated porous medium with cross-diffusion and radiative heat transfer. *Int. J Physical Sciences*, 6, pp. 4910-4923.

[5] Awad, F.G.; Sibanda, P. & Narayana, M. (2011). *Heat and mass transfer from an inverted cone in a porous medium with cross-diffusion effects*. Mass Transfer-Advanced Aspects. pp. 81-106. InTech Open Access Publisher, Croatia.

[6] Bidin, B. & Nazar, R. (2009). Numerical solution of the boundary layer flow over an exponentially stretching sheet with thermal radiation. *Euro J. Sci. Res*, 33(4), pp. 710-717.

[7] Canuto, C.; Hussaini, M. Y.; Quarteroni, A. & Zang, T. A. (1988). *Spectral Methods in Fluid Dy- namics*. Springer-Verlag, Berlin.

[8] Don, W. S. & Solomonoff, A. (1995). Accuracy and speed in computing the Chebyshev collocation derivative. *SIAM J. Sci. Comput*, 16, pp. 1253-1268.

[9] Dulal, P. (2010). Mixed convection heat transfer in the boundary layers on an exponentially stretching surface with magnetic field. *App. Math. and Com*, 217, pp. 2356-2369.

[10] Dursunkaya, Z. & Worek, W. M. (1992). Diffusion-thermo and thermal diffusion effects in transient and steady natural convection from a vertical surface. *Int. J. Heat Mass Transfer*, 35, pp. 2060 -2065.

[11] Eckeret, E. R. G. & Drake, R. M. (1972). *Analysis of heat and mass transfer*. McGraw-Hill, New York.

[12] El-Aziz, M. A. (2008). Thermal-diffusion and diffusion-thermo effects on combined heat mass transfer by hydromagnetic three-dimensional free convection over a permeable stretching surface with radiation. *Physics Letter A*, 372, pp. 263-272.

[13] Elbashbeshy, E. M. A. (2001). Heat transfer over an exponentially stretching continuous surface with suction. *Archive of Mechanics*, 53, pp. 643-651.

[14] Ibrahim, S. Y. & Makinde, O. D. (2010). Chemically reacting MHD boundary layer flow of heat and mass transfer past a moving vertical plate with suction. *Scientific Research and Essay*, 5, pp. 2875-2882.

[15] Ishak, A. (2011). MHD boundary layer flow due to an exponentially stretching sheet with radiation effect. *Sains Malaysiana*, 40, pp. 391-395.

[16] Javed, T.; Sajid, M.; Abbas, Z. & Ali, N. (2011). Non-similar solution for rotating flow over an exponentially stretching surface. *Int. J. Numerical Methods for Heat and Fluid Flow*, 21, pp. 903-908.

[17] Khan, S. K. (2006). Boundary layer viscoelastic fluid flow over an exponentially stretching sheet. *International Journal of Applied Mechanics and Engineering*, 11, pp. 321-335.

[18] Loganathan, P.; Iranian, D. & Ganesan, P. (2011). Effects of chemical reaction on unsteady free convection and mass transfer flow past a vertical plate with variable viscosity and thermal conductivity. *European J. of Sc. Research*, 59, pp. 403-416.

[19] Magyari, E. & Keller, B. (1999). Heat and mass transfer in the boundary layers on an exponentially stretching continuous surface. *J Phys D: Appl Phy*, 32, pp. 577-585.

[20] Makukula, Z. G.; Sibanda, P. & Motsa, S. S. (2010). A note on the solution of the Von Kármán equations using series and chebyshev spectral methods. *Boundary Value Problems*, ID 471793 (2010).

[21] Makukula, Z.G.; Sibanda, P. & Motsa, S. S. (2010). On new solutions for heat transfer in a visco-elastic fluid between parallel plates. *Internationl Journal of Mathematical Models and Method in Applied Sciences*, 4, pp. 221-230.

[22] Makukula, Z.G.; Sibanda, P. & Motsa, S. S. (2010). A novel numerical technique for two-dimensional laminar flow between two moving porous walls. *Mathematical Problems in Engineering*, 2010, Article ID 528956. doi:10.1155/2010/528956.

http://dx.doi.org/10.5772/55320

[23] Motsa, S. S.; Sibanda, P. & Shateyi, S. (2011). On a new quasi-linearization method for systems of nonlinear boundary value problems. *Mathematical Methods in the Applied Sciences*, 34, pp. 1406-1413.

[24] Partha, M. K.; Murthy, P. V. S. N. & Rajasekhar, G. P. (2005). Effect of viscous dissipation on the mixed convection heat transfer from an exponentially stretching surface. *Heat Mass Transfer*, 41, pp. 360-366.

[25] Partha, M. K.; Murthy, P. V. S. N. & Rajasekhar, G. P. (2006). Soret and Dufour effects in a non-Darcy porous medium. *J. Heat Transfer*, 128, pp. 605-610.

[26] Raptis, A. (1998). Radiation and free convection flow through a porous medium. *International Communications in Heat and Mass Transfer*, 25, pp. 289-295.

[27] Sparrow, E.M. & Cess, R.D. (1978). *Radiation Heat Transfer*. Hemisphere, Washington.

[28] Sajid, M. & Hayat, T. (2009). Influence of thermal radiation on the boundary layer flow due to an exponentially stretching sheet. *Int. Comm. Heat Mass Transfer*, 35, pp. 347-356.

[29] Sanjayanand, E. & Khan, S. K. (2006). On heat and mass transfer in a viscoelastic boundary layer flow over an exponentially stretching sheet. *International Journal of Thermal Sciences*, 45, pp. 819-828.

[30] Sakiadis, B.C. (1961). Boundary layer behavior on continuous solid surfaces I: Boundary layer equations for two dimensional and axi-symmetric flow. *AIChE J*, 7, pp. 26-28.

[31] Sakiadis, B.C. (1976). Boundary layer behavior on continuous solid surfaces II. The boundary layer on a continuous flat surfaces. *AIChE J*, 7, pp. 221-225.

[32] Shateyi, S. & Motsa, S.S. (2010). Variable viscosity on magnetohydrodynamic fluid flow and heat transfer over an unsteady stretching surface with hall effect. *Boundary Value Problems*, 2010, Article ID 257568. doi:10.1155/2010/257568.

[33] Srinivasacharya, D. & RamReddy, Ch. (2011). Soret and Dufour Effects on Mixed Convection from an Exponentially Stretching Surface. *Int. J of Nonlinear Science*, 12, pp. 60-68.